

AD-A159 025

A METHOD TO DETERMINE DYNAMIC ELASTIC CONSTANTS OF THIN SHELL COMPOSITES B (U) NAVAL SURFACE WEAPONS CENTER
SILVER SPRING MD J V FOLTZ ET AL 15 JUN 85

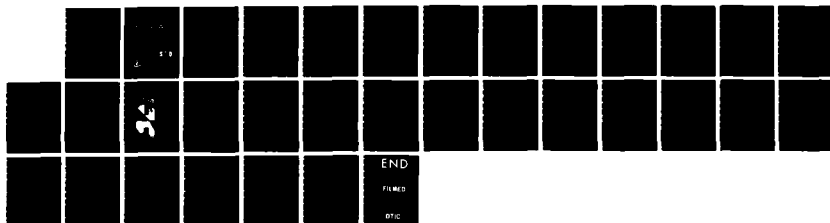
1/1

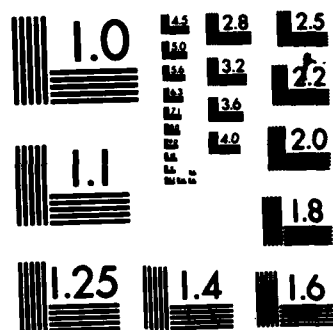
UNCLASSIFIED

NSWC/TR-85-186

F/G 11/4

NL





MICROCOPY RESOLUTION TEST CHART
NATIONAL BUREAU OF STANDARDS-1963-A

2

NSWC TR 85-186

AD-A159 025

A METHOD TO DETERMINE DYNAMIC ELASTIC CONSTANTS OF THIN SHELL COMPOSITES BY GUIDED ULTRASONIC WAVES

BY J. V. FOLTZ, A. L. BERTRAM, C. W. ANDERSON

MATERIALS DIVISION

15 JUNE 1985

Approved for public release; distribution is unlimited.

DTIC
ELECTE
SEP 12 1985
S E D

FILE COPY



NAVAL SURFACE WEAPONS CENTER

Dahlgren, Virginia 22448 • Silver Spring, Maryland 20910

85 9 09 062

UNCLASSIFIED

SECURITY CLASSIFICATION OF THIS PAGE (When Data Entered)

REPORT DOCUMENTATION PAGE		READ INSTRUCTIONS BEFORE COMPLETING FORM
1. REPORT NUMBER NSWC TR 85-186	2. GOVT ACCESSION NO. AD-A159025	3. RECIPIENT'S CATALOG NUMBER
4. TITLE (and Subtitle) A METHOD TO DETERMINE DYNAMIC ELASTIC CONSTANTS OF THIN SHELL COMPOSITES BY GUIDED ULTRASONIC WAVES		5. TYPE OF REPORT & PERIOD COVERED
		6. PERFORMING ORG. REPORT NUMBER
7. AUTHOR(s) J. V. Foltz, A. L. Bertram, C. W. Anderson		8. CONTRACT OR GRANT NUMBER(s)
9. PERFORMING ORGANIZATION NAME AND ADDRESS Naval Surface Weapons Center 10901 New Hampshire Avenue Silver Spring, MD 20903-5000		10. PROGRAM ELEMENT, PROJECT, TASK AREA & WORK UNIT NUMBERS 62761N, SF61-543-694, 5R37BC
11. CONTROLLING OFFICE NAME AND ADDRESS		12. REPORT DATE 15 June 1985
		13. NUMBER OF PAGES 34
14. MONITORING AGENCY NAME & ADDRESS (if different from Controlling Office)		15. SECURITY CLASS. (of this report) UNCLASSIFIED
		15a. DECLASSIFICATION/DOWNGRADING SCHEDULE
16. DISTRIBUTION STATEMENT (of this Report) Approved for public release; distribution is unlimited.		
17. DISTRIBUTION STATEMENT (of the abstract entered in Block 20, if different from Report)		
18. SUPPLEMENTARY NOTES		
19. KEY WORDS (Continue on reverse side if necessary and identify by block number) Metal Matrix Composites Guided Ultrasonic Waves		
20. ABSTRACT (Continue on reverse side if necessary and identify by block number) Advanced composite materials are frequently used as plate or shell structural members having four in-plane elasticity parameters. This work documents a method for obtaining these elastic constants using guided ultrasonic waves. Metal matrix composite plates are used to provide examples of the approach.		

FOREWORD

→ Ultrasonic techniques are used to determine the velocities of guided waves in unidirectional metal matrix composite plates. Both extensional (fundamental Lamb symmetric) and in-plane shear (SH) plate wave speeds are measured via through-transmission procedures utilizing one-half megahertz broadband transducers. The values recorded for the wave speeds and the plate density are used to calculate the four reduced stiffness coefficients of the plane stress Hooke's Law relationship of the plate. This approach allows the full set of elastic constants required by designers for the analysis of a thin orthotropic plate or shell loaded in its plane to be obtained from only four ultrasonic measurements. The accuracy of the elastic constant determinations may be increased by measuring more than four wave speeds and employing the statistical data reduction method described herein.

Approved by:

J. R. Dixon
J. R. DIXON, Head
Materials Division

Accession For	
NTIS GRA&I	<input checked="" type="checkbox"/>
DTIC TAB	<input type="checkbox"/>
Unannounced	<input type="checkbox"/>
Justification	
By	
Distribution/	
Availability Codes	
Dist	Avail and/or Special
A-1	



CONTENTS

	<u>Page</u>
INTRODUCTION	1
REVIEW OF THEORY	1
EXPERIMENTAL	8
DISCUSSION	16
CONCLUSIONS	16
RECOMMENDATIONS	16
REFERENCES	17

APPENDIX

A	COMPUTER PROGRAM FOR CALCULATING PLATE WAVE SPEEDS FROM ELASTIC CONSTANTS	A-1
B	PROGRAM FOR CALCULATING LAMINA STIFFNESS COEFFICIENTS FROM PLATE WAVE SPEEDS	B-1

ILLUSTRATIONS

<u>Figure</u>		<u>Page</u>
1	DEFLECTED ACOUSTIC BEAM TRAJECTORY IN AN ANISOTROPIC PLATE	7
2	BORON/ALUMINUM SPECIMENS	10
3	POINT-SOURCE TRANSDUCER EXCITING LONGITUDINAL TYPE PLATE WAVES	14
4	GROUP VELOCITY ENVELOPE FOR WAVES IN GY70/A201	15
B-1	LEAST-SQUARE-ERROR CURVES VS MEASURED PLATE WAVE SPEEDS FOR BORON/ALUMINUM	B-5

TABLES

<u>Table</u>		<u>Page</u>
1	DESCRIPTION OF PLATES USED IN ULTRASONIC STUDIES	9
2	BORON/ALUMINUM UNIDIRECTIONAL LAMINA PLATE WAVE VELOCITIES AND ACOUSTICAL PRESSURES	12
3	GRAPHITE/ALUMINUM UNIDIRECTIONAL LAMINA PLATE WAVE VELOCITIES AND ACOUSTICAL PRESSURES	12
4	BORON/ALUMINUM UNIDIRECTIONAL LAMINA ELASTIC CONSTANTS	13
5	GRAPHITE/ALUMINUM UNIDIRECTIONAL LAMINA ELASTIC CONSTANTS	13
A-1	CALCULATED PLATE WAVE SPEEDS OF GY70/A201	A-4
B-1	REDUCED STIFFNESS COEFFICIENTS OF B/A ₂ FROM PLATE WAVE DATA	B-4

INTRODUCTION

Metal Matrix Composites (MMCs) are a class of structural materials that has attractive features for many applications. Lightweight MMCs (based primarily on the addition of a reinforcement to an aluminum or magnesium matrix) are being developed for structural members such as shells, shelves, and stiffeners. For this generic type of element the thickness is usually much smaller than the other dimensions. Typically, an MMC shell component is no more than 2.5mm thick with the other dimensions being at least one order of magnitude greater.

Nondestructive inspection of such members frequently relies on ultrasonics as a tool. A geometry in which one dimension of a part is significantly smaller than the other two is well suited to the use of plate modes of ultrasonic wave propagation. With the ready availability of ceramic transducers that have operating frequencies in the range of 1/2 to 1 megahertz the inspection of thin sheet and shell members by plate waves is a practical approach. In addition to flaw detection, a full set of in-plane material elastic constants may be obtained from the measurements of the proper plate wave velocities. The purpose of this note is to summarize and catalogue the first-order equations which express plate wave velocities as functions of the elastic constants and density of an orthotropic laminate. In addition, the method by which elastic constants are determined from phase velocity measurements is reviewed. In practice, experimental measurements often garner more wavespeed data than are needed to algebraically solve the pertinent equations. This problem of over determination of variables is addressed via regressive analysis. Some simple examples are presented using unidirectional boron/aluminum (B/Al) and graphite/aluminum (Gr/Al) as representative MMCs.

REVIEW OF THEORY

It is known that the propagation speed of an ultrasonic wave in anisotropic media is a function of the material elastic constants and density. For single crystals, the elastic constants may be unambiguously defined. For two-phase materials, such as structural composites, an appropriate model of media response to a transient elastic disturbance must be adopted in order to quantify the relationship between wave velocities and elastic constants. When the effective wavelength of the acoustic pulse is much larger than the dimensions of the microstructural inhomogeneities, the effective modulus theory has been applied

for this purpose. Examples in the literature demonstrate the application of effective modulus theory to relate ultrasonic parameters to material properties for a variety of composites. A summary of the relevant equations for the two plate modes (P waves and SH waves) of present interest is presented herein.

The effective modulus theory assumes that a composite material is a macroscopically homogeneous, orthotropic medium. For thin shell geometries the further assumption of a plane stress state is frequently adopted. Under these conditions, the Hooke's law relationship between stress and strain is written

$$\begin{pmatrix} \sigma_1 \\ \sigma_2 \\ \tau_{12} \end{pmatrix} = \begin{pmatrix} Q_{11} & Q_{12} & 0 \\ Q_{12} & Q_{22} & 0 \\ 0 & 0 & Q_{66} \end{pmatrix} \begin{pmatrix} \epsilon_1 \\ \epsilon_2 \\ \gamma_{12} \end{pmatrix} \quad (1)$$

if the stresses ($\sigma_1, \sigma_2, \tau_{12}$) and the strains ($\epsilon_1, \epsilon_2, \gamma_{12}$) are indexed to a cartesian coordinate system aligned with the laminate principal axes.

The problem of determining the velocity of waves propagating in an isotropic plate was originally solved by Lamb. Among other things, the results showed that two basic families of waves could propagate, one having symmetrical and one unsymmetrical characteristics. The long-wavelength (where the wavelength is measured in units of plate thickness) symmetrical mode is mildly dispersive, with the approximate wavespeed being a simple function of the plate moduli and density. The antisymmetrical mode is highly dispersive. For the symmetrical Lamb wave, as the wavelength becomes infinitely long, the limiting velocity is referred to as the extensional plate velocity. Subsequent work by other investigators developed similar plate velocity expressions for orthotropic elastic plates. The extensional plate wave velocity and its shear mode analogue may be expressed as functions of the elastic constants of a composite laminate by using Equation (1) in conjunction with the equations of motion of the laminate material as it is disturbed by the ultrasonic wavefront. A simple derivation, based on a time-harmonic wave train, is summarized here.

A field point in the laminate located at coordinates (x,y) oscillates with respective displacements (u,v). The strains at (x,y) are then

$$\begin{aligned} \epsilon_1 &= \frac{\partial u}{\partial x} \\ \epsilon_2 &= \frac{\partial v}{\partial y} \\ \gamma_{12} &= \frac{\partial u}{\partial y} + \frac{\partial v}{\partial x} \end{aligned} \quad (2)$$

When the wavelength of the disturbance is much greater than the laminate thickness plate wave modes are activated and, for the lowest order of P wave and SH wave, the displacement at (x,y) may be approximated as uniform across the plate thickness. The displacements due to a harmonic wave will vary with time, t, as

$$u = u_0 \exp[i(k x \cos \theta + k y \sin \theta - \omega t)] \quad (3)$$

A similar expression exists for v . In Equation (3), ω is the angular frequency, $k = \omega/V$, where V is the phase velocity of the wave, and θ is the angle between the x axis and the normal to the wavefront.

From Newton's laws, the equation of motion of the field point is

$$\left(\frac{\partial \sigma_1}{\partial x}\right) + \left(\frac{\partial \tau_{12}}{\partial y}\right) = \rho \left(\frac{\partial^2 u}{\partial t^2}\right) \quad (4)$$

$$\left(\frac{\partial \sigma_2}{\partial y}\right) + \left(\frac{\partial \tau_{12}}{\partial x}\right) = \rho \left(\frac{\partial^2 v}{\partial t^2}\right)$$

In Equation (4), ρ is the composite density.

Combining Equations (1) through (4) yields the Christoffel equation for (u_0, v_0) , which is solved by setting the characteristic determinant equal to zero. This relationship is known as the dispersion equation, Equation (5).

$$\begin{vmatrix} A_{11} - \chi & A_{12} \\ A_{12} & A_{22} - \chi \end{vmatrix} = 0 \quad (5)$$

In Equation (5), $\chi = \rho V^2$ and the A_{ij} parameters are functions of the laminate stiffness coefficients, Q_{ij} , and the direction of wave propagation, θ , as follows:

$$\begin{aligned} A_{11} &= Q_{11} \cos^2 \theta + Q_{66} \sin^2 \theta \\ A_{22} &= Q_{66} \cos^2 \theta + Q_{22} \sin^2 \theta \\ A_{12} &= (Q_{12} + Q_{66}) \sin \theta \cos \theta \end{aligned} \quad (6)$$

Mathematically, Equation (5) is a quadratic with two roots for each angle θ . The larger root, representing the faster wave, χ_F , is

$$\chi_F = \left(\frac{A_{11} + A_{22}}{2} \right) + \left(\frac{\sqrt{(A_{11} - A_{22})^2 + 4 A_{12}^2}}{2} \right) \quad (7)$$

The smaller root, corresponding to the slower wave, χ_s , is obtained by changing the plus sign between the two terms of Equation (7) to a minus sign.

The physical interpretation of the two roots is that in any direction in the plane of the lamina two types of waves may propagate which involve principally in-plane stresses. Neither type will generate a net moment as, for example, does a wave of flexure. These waves become pure mode longitudinal and pure mode shear only when the propagation direction is along a laminate principal axis. For these directions $\theta = 0^\circ$ or $\theta = 90^\circ$ and the phase velocities are

$$\begin{aligned}
 V_F(0^\circ) &= \sqrt{Q_{11}/\rho} \\
 V_F(90^\circ) &= \sqrt{Q_{22}/\rho} \\
 V_S(0^\circ) &= V_S(90^\circ) = \sqrt{Q_{66}/\rho}
 \end{aligned}
 \tag{8}$$

For off-axis waves the mode is not pure and the terms pseudo-longitudinal waves and pseudo-shear waves are sometimes used as descriptors. The relationships between the Q_{ij} coefficients and the conventional engineering elastic constants (Young's moduli, shear modulus, and Poisson's ratios) are:

$$\begin{aligned}
 Q_{11} &= E_{11}/(1 - \nu_{12} \nu_{21}) \\
 Q_{22} &= E_{22}/(1 - \nu_{12} \nu_{21}) \\
 Q_{12} &= \nu_{12} Q_{22} \\
 Q_{66} &= G_{12} \\
 \nu_{21} E_{11} &= \nu_{12} E_{22}
 \end{aligned}
 \tag{9}$$

In Equation (9), E_{11} and E_{22} are the extensional moduli in directions x and y , respectively; ν_{12} and ν_{21} are the major and minor Poisson's ratios; and G_{12} is the in-plane shear modulus.

In order to check the predictions of these equations a panel of orthotropic material with known elastic constants is needed. Given the set of four elastic parameters plus the panel density, the phase velocities of the two types of waves may be calculated from Equation (8) and compared to the experimental measurements in the principal directions. Off-axis waves may also be used for this purpose but greater care must be taken to ensure that the correct mode is observed due to certain directional propagation effects present in orthotropic media, as discussed below.

Acoustical birefringence occurs in anisotropic media. That is, the phase velocity varies with direction. Even when using a model of material behavior that neglects dependence of phase velocity on frequency, the directional variation of V leads to the existence of a wave modulation envelope which travels with a group velocity, V_G , that is not always the same as the phase velocity. The group velocity is a vector and its components in the x and y directions are

$$\begin{aligned}
 V_{Gx} &= \frac{\partial \omega}{\partial k_x} \\
 V_{Gy} &= \frac{\partial \omega}{\partial k_y}
 \end{aligned}
 \tag{10}$$

In Equation (10), $k_x = k \cos \theta$ and $k_y = k \sin \theta$. The partial derivatives are determined by implicit differentiation of the dispersion relation, Equation (5). This relation written in expanded form is

$$\Omega(\omega, k_x, k_y) = (k_x^2 Q_{11} + k_y^2 Q_{66} - \rho\omega^2) (k_x^2 Q_{66} + k_y^2 Q_{22} - \rho\omega^2) - (k_x k_y (Q_{12} + Q_{66}))^2 = 0$$

The components of V_G may be expressed

$$V_{Gx} = - \frac{\partial \Omega / \partial k_x}{\partial \Omega / \partial \omega}$$

$$V_{Gy} = - \frac{\partial \Omega / \partial k_y}{\partial \Omega / \partial \omega}$$
(11)

The corresponding partial derivatives are

$$\begin{aligned} \frac{\partial \Omega}{\partial k_x} &= (k_x^2 Q_{11} + k_y^2 Q_{66} - \rho\omega^2)(2 k_x Q_{66}) \\ &+ (k_x^2 Q_{66} + k_y^2 Q_{22} - \rho\omega^2)(2 k_x Q_{11}) - 2 k_x k_y^2 (Q_{12} + Q_{66})^2 \end{aligned}$$
(12)

$$\begin{aligned} \frac{\partial \Omega}{\partial k_y} &= (k_x^2 Q_{11} + k_y^2 Q_{66} - \rho\omega^2)(2 k_y Q_{22}) \\ &+ (k_x^2 Q_{66} + k_y^2 Q_{22} - \rho\omega^2)(2 k_y Q_{66}) - 2 k_x^2 k_y (Q_{12} + Q_{66})^2 \end{aligned}$$
(13)

$$\frac{\partial \Omega}{\partial \omega} = (k_x^2 (Q_{11} + Q_{66}) + k_y^2 (Q_{22} + Q_{66}) - 2\rho\omega^2)(-2\rho\omega)$$
(14)

The direction of group velocity advancement with respect to the x axis, θ_G , is found from

$$\tan \theta_G = \frac{\text{Equation (13)}}{\text{Equation (12)}}$$
(15)

The magnitude of V_G is

$$V_G^2 = \frac{[\text{Equation (12)}]^2 + [\text{Equation (13)}]^2}{[\text{Equation (14)}]^2}$$
(16)

In Equation (15), θ_G is the angle of inclination of the group velocity propagation direction for an ultrasonic wave packet that is launched with a phase velocity propagation direction of angle θ . Solution of Equation (15) shows that $\theta_G = \theta$ only for the two angles 0° and 90° .

The fact that for off-axis waves the phase and group velocities do not advance in the same direction is important to properly sizing a specimen for measurement of off-axis phase velocities. When a pulse of acoustical energy is radiated by a plane wave transducer, the phase front is aligned parallel to the transducer face. However, the energy propagates in the direction of the group

velocity, which is not normal to the transducer face. The angle of energy cant from the transducer normal may be significant and, for a through-transmission type of wave speed measurement, can lead to improper placement of the receiving transducer. The specimen dimensions must be large enough to account for this canting effect so that the receiver may be offset by the proper amount to intercept the pulse. Figure 1 depicts schematically the beam deflection phenomenon for an off-axis wave propagating in a directional media. From the figure, the phase velocity is numerically equal to the perpendicular distance separating the transducers, L , divided by the time of flight of the group wave packet. Also, note that

$$V = V_G \cos(\theta_G - \theta) \quad (17)$$

A number of investigators have used measured phase velocities to calculate the elastic constants of a composite. In the present formulation, this problem reduces to determining the four stiffness parameters-- Q_{11} , Q_{22} , Q_{66} , Q_{12} --from measured plate velocities. Therefore, a minimum of four velocities must be recorded. At least one value is needed in an off-axis direction or v_{12} cannot be determined. Algebraic solution of Equation (7) from the four experimental quantities plus the density is then possible. A convenient approach is to interrogate a specimen at $\theta=0^\circ$ and $\theta=90^\circ$, since for these directions the phase velocity propagates normal to the transducer face. The influence of Poisson's ratio on wave speed derives largely from the effect of the magnitude of A_{12} on the calculated results of Equation (7). The value of A_{12} is proportional to the product $\sin\theta \cos\theta$, which is a maximum at $\theta=45^\circ$. Therefore, it is advisable to determine at least one wave speed at $\theta=\pi/4$, if possible.

At times, more than four experimental wave speed values are available. When this situation occurs, the accuracy of the Q_{ij} determinations may be increased by using the method of non-linear least square error analysis. The approach is to fit the two curves defined by Equation (7) to the total set of data in such a way that the sum of the absolute deviations of the data points from the smooth curves is a minimal. The following discussion assumes that the experimental error in wave speed measurement is the same for all data points.

From Equation (7), two curves represent the behavior of both in-plane plate wave modes, where the curve parameters are X_F and X_S expressed as functions of the four Q_{ij} 's and θ . The goodness of fit of a set of data to these two curves, δ , is defined as

$$\delta = \sum_n \left\{ (X_F - X_1)^2 + (X_S - X_2)^2 \right\} \quad (18)$$

Equation (18) is a summation over all specimen angles interrogated, n . In Equation (18), $X_F = X_F(Q_{ij}, \theta_n)$ and $X_1 = \rho V_F^2$, where V_F is the measured speed of the faster wave for angle θ_n . Similarly, $X_S = X_S(Q_{ij}, \theta_n)$ and $X_2 = \rho V_S^2$ at angle θ_n .

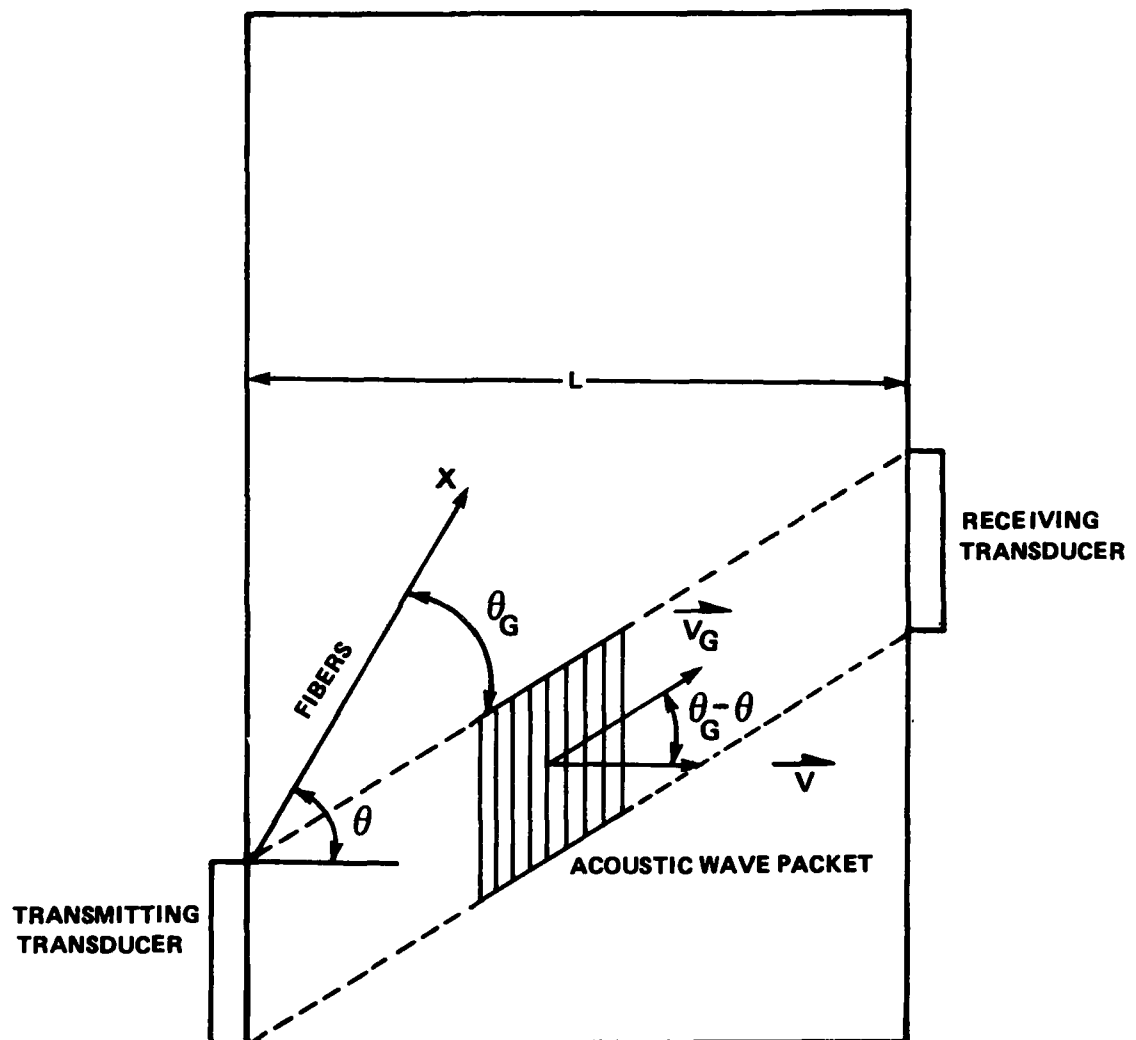


FIGURE 1. DEFLECTED ACOUSTIC BEAM TRAJECTORY IN AN ANISOTROPIC PLATE

The function δ is here considered a continuous function of the four unknown Q_{ij} 's; each Q_{ij} is an independent variable. Thus δ describes a hyper-surface in four-dimensional Q_{ij} space and the space must be searched for the minimum value of δ . The search procedure consists of establishing a four-dimensional grid mapping of the area of Q_{ij} space in which δ is suspected to be minimal, and then progressively tightening the grid by reducing the range of values of each of the Q_{ij} 's.

In the simplest mapping procedure, the permissible range for each Q_{ij} is divided into two equal increments about its median value. The mid-range point plus the two extremities constitute three trial values for each Q_{ij} so that the 4-parameter space is divided into a grid consisting of 81 vertices. The value of δ is then calculated at each of these vertices. This procedure yields a map of the behavior of δ as a function of all of the Q_{ij} parameters. The grid may be made initially very coarse on a "best guess" basis, and then, when a local minimum is identified, made finer by adjusting the median value of each Q_{ij} and reducing the incremental offset about the mid-point.

Computer programs in BASIC for calculating the phase and group velocities from laminate elastic constants and density and for determining the best-fit set of Q_{ij} 's from a collection of experimental phase velocities are included in this report as Appendices A and B, respectively.

EXPERIMENTAL

Two types of MMC were available for preliminary evaluation of the preceding theory. Both consisted of unidirectionally reinforced aluminum in a thin lamina form and are therefore characterized with respect to in-plane stiffness behavior by four independent elastic constants-- E_{11} , the axial elastic modulus; E_{22} , the transverse elastic modulus; ν_{12} , the major Poisson's ratio; and G_{12} , the in-plane shear modulus. Some physical properties of the as-received plates are given in Table 1. The boron filament used in B/Al is a product of AVCO; the precursor wire of which the plate of Gr/Al is made was manufactured by Material Concepts, Inc. Plate consolidation was performed by DWA Composite Specialties in both cases. Although similar in regard to matrix type and reinforcement arrangement, the boron filament and graphite fiber differ in average diameter by approximately one order of magnitude. Thin panels of these kinds can serve as structural materials in their unidirectional form or as the unit of construction for complex laminate layups.

The experimental approach was to cut the panels into various sample sizes for measurement of ultrasonic phase velocities by through-transmission methods. Figure 2 shows three typical samples of B/Al. Both longitudinal-type waves and in-plane shear waves were studied using broadband transducers which had a nominal 0.5 MHz center frequency. The materials were interrogated to determine the velocities of both types of waves at five angles with respect to the reinforcement direction. Densities were obtained by immersion. The resulting

TABLE 1. DESCRIPTION OF PLATES USED IN ULTRASONIC STUDIES

	Length (cm)	Width (cm)	Thickness (cm)
Boron/Al ^a	23.8	7.6	0.138
Graphite/Al ^b	30.0	30.0	0.068

	Filament Type	Alloy	Reinforcement Fraction	Density (gm/cm ³)
Boron/Al ^a	5.6-mil boron	6061	0.51	2.59
Graphite/Al ^b	GY-70 graphite	A201	0.37	2.52

a. DWA Plate No. B-1379-1

b. DWA Plate No. G-5100

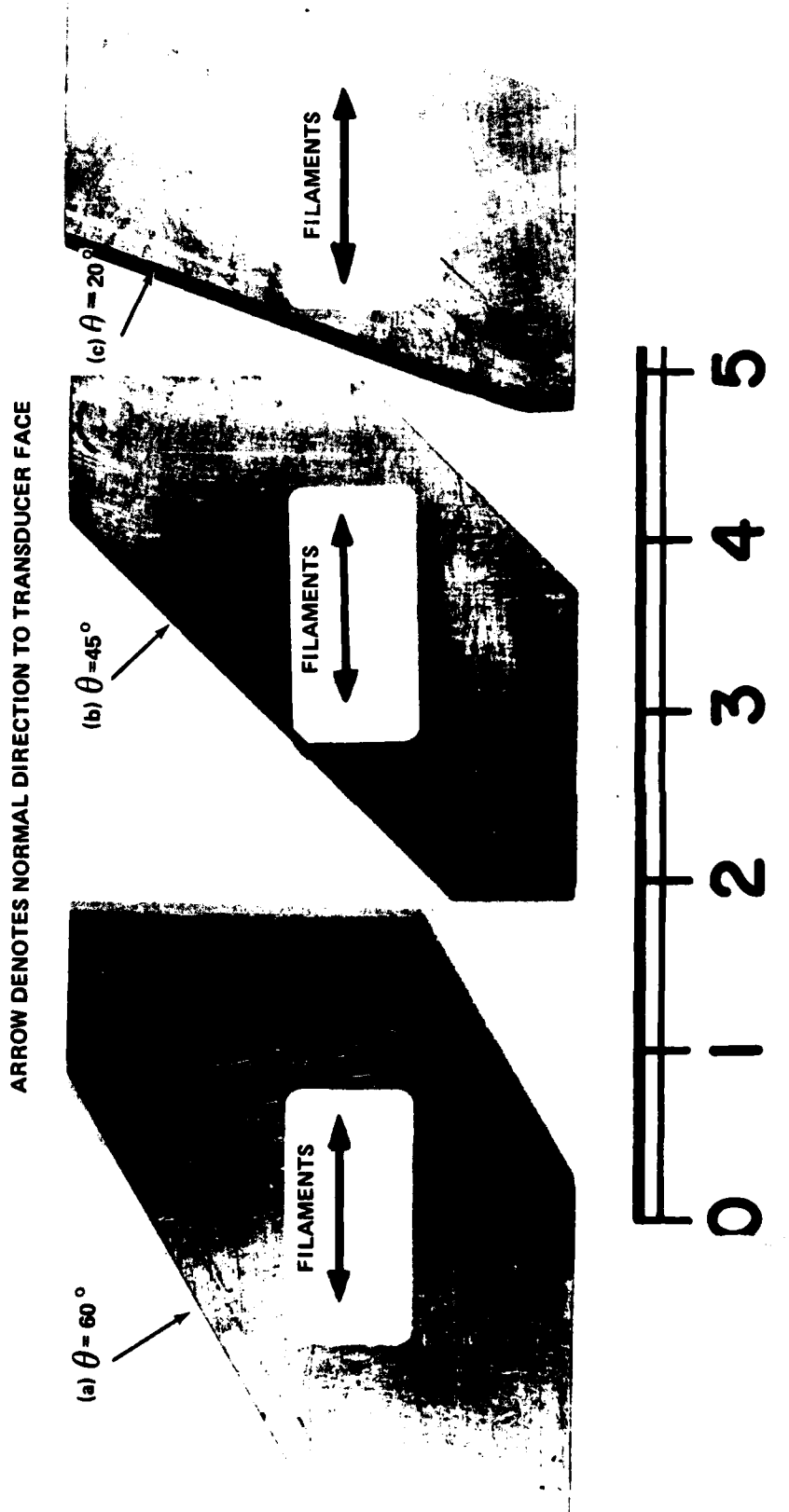


FIGURE 2. BORON/ALUMINUM SPECIMENS

velocities and calculated values of X_F and X_S are presented in Tables 2 and 3. The composite elastic constants were obtained for each material by applying the least-square-error program of Appendix B. These values are listed in Tables 4 and 5.

The B/Al plate was not large enough to permit additional mechanical tests to be conducted which would provide comparative data for the elastic constants. Therefore, the results of an investigation in the literature is utilized for this purpose, Reference 1. In this study the complete orthotropic elastic-stiffness matrix of unidirectional, Borsic-filament-reinforced Al composites was experimentally evaluated for three different volume fractions by ultrasonic bulk wave velocity measurements. The fiber-volume fractions reported are 0.13, 0.34 and 0.54. Interpolation of the elastic constants from this paper to the fiber-fraction of the B/Al plate used in the present study (0.51) gives the set of elastic constants listed in Table 4.

The Gr/Al plate was large enough to allow coupons to be cut for tensile evaluation of Young's modulus in the fiber direction, E_{11} . Three tests were performed; the results are given in Table 5. Insufficient material precluded running mechanical tests to determine the remaining three properties. Since E_{22} and G_{12} are both matrix-dominated properties, a rough estimate of their value for an aluminum composite incorporating 37% graphite may be obtained from studies on other types of unidirectional Gr/Al of approximately equal fiber fraction (References 2 and 3).

The composite cylinder assemblage model has been used to predict the properties of a Gr/Al material from calculations based on fiber and matrix constituent properties, Reference 2. Fiber fractions ranging from 0 to 50 percent were addressed in 10 percent increments, allowing interpolation to the value of 0.37. Ultrasonic evaluations based on bulk waves of a 30 volume percent Gr/Al composite were also reported, Reference 3. Both studies involved graphite filaments of another type than GY-70.* The elastic constants from these papers are reproduced in Table 5.

Predictions of ultrasonic group velocity by the effective modulus theory were in part evaluated by an experiment which delineated the group propagation envelope directly. A small source of extensional waves was applied to one edge of the GY70/A201 plate, as shown in Figure 3. A second small transducer was employed to track a constant phase point in polar fashion about the disturbance source as origin. This procedure yields a plot of V_G versus θ_G for angles ranging from 0° to 85° . The results, presented in Figure 4, correspond to the locus of the wavefront for the faster plate wave at a time of $t = 12.8 \mu\text{sec}$ after the pulse was initiated. The theoretical curve, calculated from Equation (15) and Equation (16) using the GY70/A201 moduli of Table 5, is presented on the same figure as the experimental data for comparison.

*The filament axial elastic modulus was approximately 50×10^6 psi in both studies cited. The axial modulus of GY70 is approximately 70×10^6 psi.

TABLE 2. BORON/ALUMINUM UNIDIRECTIONAL LAMINA PLATE WAVE
VELOCITIES AND ACOUSTICAL PRESSURES

θ	V_F (mm/ μ sec)	V_S (mm/ μ sec)	X_F (GPa)	X_S (GPa)
0°	9.624	4.741	239.52	58.126
20°	9.207	4.859	219.21	61.055
45°	8.142	5.300	171.43	72.641
60°	7.946	5.274	163.28	71.930
90°	7.826	4.820	158.38	60.079

TABLE 3. GRAPHITE/ALUMINUM UNIDIRECTIONAL LAMINA PLATE WAVE
VELOCITIES AND ACOUSTICAL PRESSURES

θ	V_L (mm/ μ sec)	V_S (mm/ μ sec)	X_F (GPa)	X_S (GPa)
0°	8.84	2.74	196.9	18.92
30°	7.49	2.90	141.4	21.19
45°	6.41	2.96	103.5	22.08
60°	5.06	3.11	64.52	24.37
90°	3.88	2.75	37.93	19.06

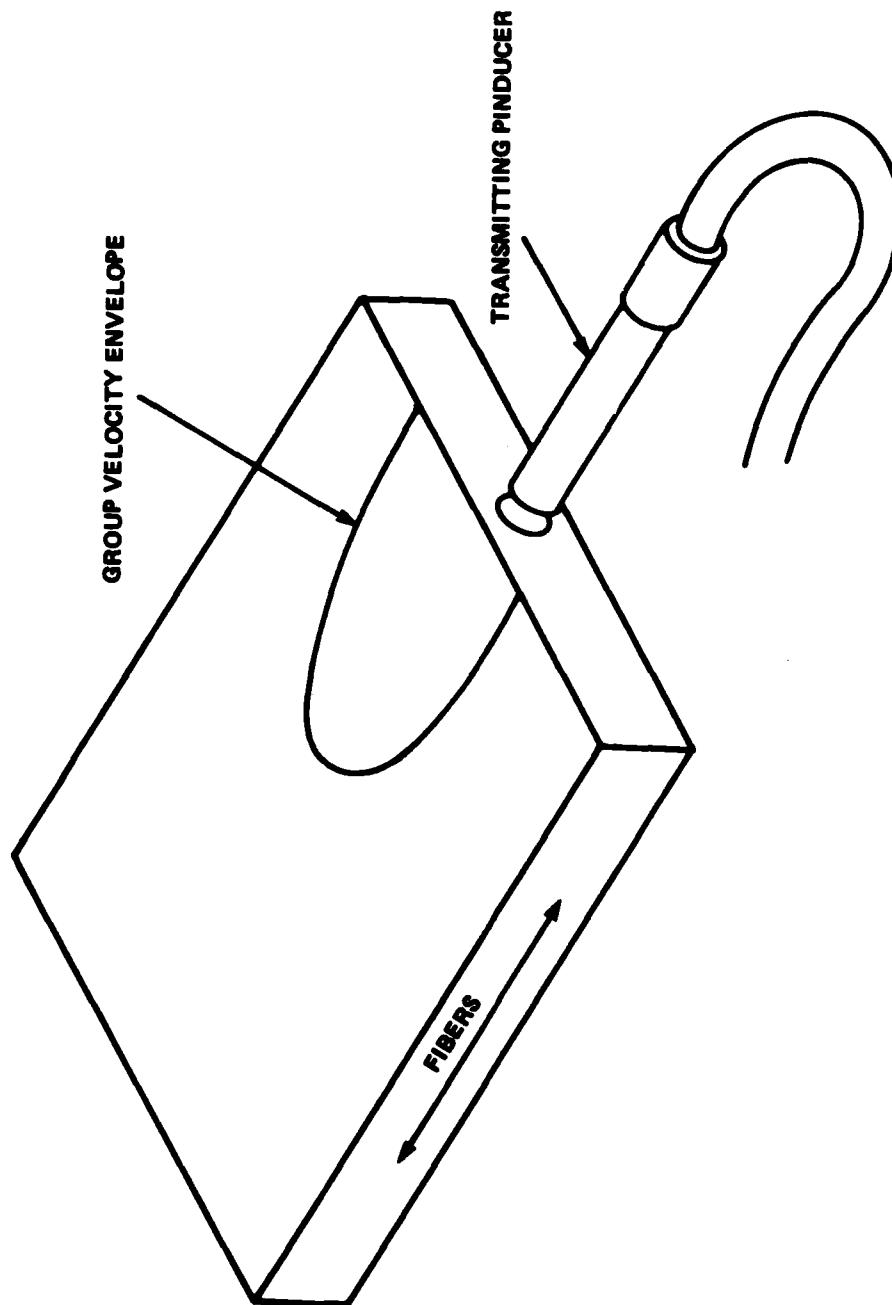


FIGURE 3 POINT-SOURCE TRANSDUCER EXCITING LONGITUDINAL-TYPE PLATE WAVES

TABLE 4. BORON/ALUMINUM UNIDIRECTIONAL LAMINA ELASTIC CONSTANTS

	Plate Waves ^a	Ref. 1 ^b
E ₁₁ (msi)	32.8	32.6
E ₂₂ (msi)	21.9	19.3
G ₁₂ (msi)	8.2	8.4
ν_{12}	0.24	0.25

- (a) 51 v/o Boron/6061
 (b) 52 v/o Borsic/6061

TABLE 5. GRAPHITE/ALUMINUM UNIDIRECTIONAL LAMINA ELASTIC CONSTANTS

	Plate Waves ^a	Tensile Test ^a	Ref. 2 ^b	Ref. 3 ^c
E ₁₁ (msi)	27.4	27.0, 29.3, 27.6	26.6	23.3
E ₂₂ (msi)	5.0	---	5.1	4.3
G ₁₂ (msi)	2.5	---	3.1	2.8
ν_{12}	0.26	---	0.34	0.28

- (a) 37 v/o GY70/A201
 (b) mathematical model predictions for 37 v/o P55/6061
 (c) 30 v/o T50/A201

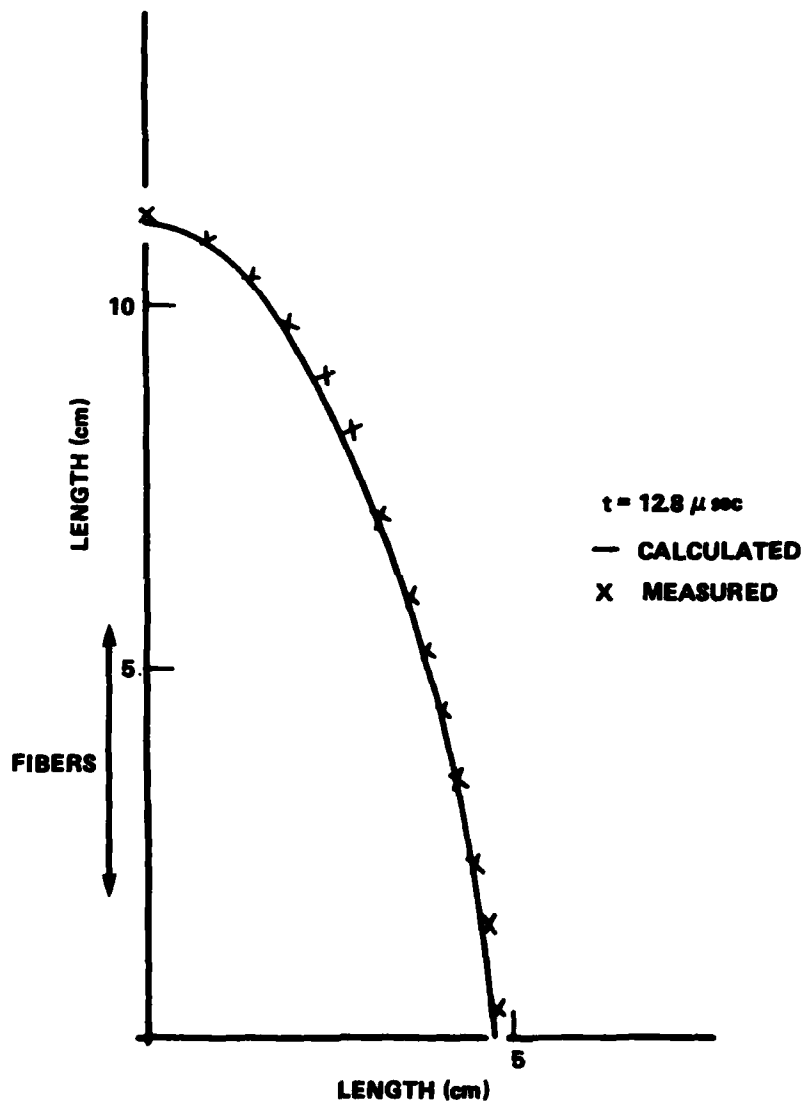


FIGURE 4. GROUP VELOCITY ENVELOPE FOR WAVES IN GY70/A201

DISCUSSION

A comparison of the elastic properties of B/Al and Gr/Al from ultrasonic plate waves with values found in the literature shows reasonable agreement for the majority of the constants. The discrepancies can be attributed to sample differences between this study and the references cited and the effect of dispersion on plate wave velocity determinations. The good agreement of plate wave values of E_{11} with the results of other types of measurement is particularly encouraging, in that axial performance of a unidirectional composite is usually of first order importance for design considerations.

Reasonable agreement is also observed between the predicted and observed group velocity envelope of an extensional-type wave generated by a point source of disturbance in Gr/Al. This fact lends confidence to the hypothesis that effective modulus theory can be applied to relate the material stiffness parameters of a unidirectional MMC to elementary elastic wave analysis.

CONCLUSIONS

Effective modulus theory appears adequate to provide a first-order approximation of in-plane plate wave propagation characteristics in thin panels and shells of unidirectional B/Al and Gr/Al. The plate wave approach appears especially relevant to determining the value of the major elastic modulus, E_{11} , which is of much interest to both users and manufacturers of MMCs.

RECOMMENDATIONS

Additional plate wave studies of the present type should be performed on other types of MMCs and on layup arrangements other than unidirectional plies. The effect of residual stresses resulting from the manufacturing process on phase velocities needs to be investigated. The development of a model of MMC material behavior with regard to transient elastic disturbances that incorporates dispersion should be addressed.

REFERENCES

1. Gieske, J. H., and Allred, R. E., "Elastic Constants of B-Al Composites by Ultrasonic Velocity Measurements," Exp. Mech., p. 158, Apr 1974.
2. "Analysis of Fabric/Metal Matrix Composites," Materials Sciences Corporation Technical Report TFR 1310/1413, Nov 1982.
3. Blessing, G. V., and Elban, W. L., "Aluminum Matrix Composite Elasticity Measured Ultrasonically," J. App. Mech., Vol. 48, p. 965, Dec 1981.

APPENDIX A

COMPUTER PROGRAM FOR CALCULATING PLATE WAVE SPEEDS
FROM ELASTIC CONSTANTS

The following computer program, written in BASIC, calculates the fundamental symmetric Lamb and SH shear plate wave velocities of an orthotropic lamina from its four elastic constants and density. Enter the input data in Step 2000 in the order:

E_{11} (Msi); E_{22} (Msi); G_{12} (Msi); ν_{12} ; and ρ (gm/cm³). A sample calculation is presented in Table A-1 using $E_{11} = 27.4$ Msi; $E_{22} = 5.0$ Msi; $G_{12} = 2.5$ Msi; $\nu_{12} = 0.26$; and $\rho = 2.52$ gm/cm³, which is a representative set of values for GY 70/A201 Gr/A1.

```

10 REM PROGRAM TO CALCULATE WAVE SPEEDS OF FUNDAMENTAL LAMB MODE
12 REM AND SH SHEAR MODE AS A FUNCTION OF ANGLE FOR THIN PLATE MATERIAL
14 REM USING THE MODULI AS INPUTS. INPUT E1(MSI),E2(MSI),G12(MSI)
16 REM POISSONS RATIO, AND DENSITY (G/CC)
17 PRINT
18 PRINT
20 PRINT "PROGRAM CALCULATIONS MADE AT 5 DEGREE INTERVALS"
60 DIM T3(95),X1(95),X2(95),Y1(95),Y2(95)
65 DIM T9(95),N9(95),Z2(95),Z3(95)
90 PRINT
102 READ E1,E2,G,V1,R
105 PRINT
106 PRINT " E1 =      ",E1,"MSI"
108 PRINT " E2 =      ",E2,"MSI"
110 PRINT " G12 =     ",G,"MSI"
112 PRINT " POISSONS RATIO = ",V1
114 PRINT " DENSITY = ",R,"GMS/CC"
115 PRINT
116 PRINT
117 PRINT "FAST WAVE SPEEDS VERSUS ANGLE"
118 PRINT
119 PRINT
120 PRINT "THETA PHASE","F PHASE VEL","THETA GROUP","F GROUP VEL"
122 PRINT "(DEGREES)","(MM/USEC)","(DEGREES)","(MM/USEC)"
124 PRINT
128 V2=V1*(E2/E1)
130 A1=E1/((1-V1*V2)*0.145)
140 A2=E2/((1-V1*V2)*0.145)
150 A3=(V2*E1)/((1-V1*V2)*0.145)
160 A6=G/.145
200 FOR I=0 TO 90 STEP 5
210 T2=I*(6.283185/360)
215 T3(I)=T2
220 L=COS(T2)
230 L2=L*L
240 M=(1-L2)**0.5
250 M2=M*M
260 H1=L2*A1+M2*A6
270 H2=L2*A6+M2*A2
280 H3=L*M*(A3+A6)
290 H4=H3*H3
300 H7=H1+H2
310 H8=H7*H7
320 H9=H1*H2-H4
400 X1=0.5*(H7+(H8-4*H9)**0.5)
410 X2=0.5*(H7-(H8-4*H9)**0.5)
420 U1=(X1/R)**0.5
600 F1=(L2*A1+M2*A6-R*U1*U1)*(2*M*A2)
610 B1=(L2*A1+M2*A6-R*U1*U1)*(2*L*A6)
620 F2=(L2*A6+M2*A2-R*U1*U1)*(2*M*A6)
630 B2=(L2*A6+M2*A2-R*U1*U1)*(2*L*A1)
640 F3=-2*M*L2*(A3+A6)**2
650 B3=-2*L*M2*(A3+A6)**2
660 F4=F1+F2+F3

```

```

670 G4=G1+G2+G3
680 U1=L2*(A1+A6)+M2*(A6+A2)-2*R*U1*U1
690 U2=-2*R*U1
700 U3=U1*U2
710 U4=(F4+F4+G4+G4)/(U3*U3)
720 U5=U4**5
730 T7=F4/G4
740 T8=(180/3.14159)*ATN(T7)
760 PRINT I,U1,T8,U5
1000 NEXT I
1010 PRINT
1020 PRINT
1022 PRINT "SLOW WAVE SPEEDS VERSUS ANGLE"
1024 PRINT
1026 PRINT
1030 PRINT "THETA PHASE","S PHASE VEL","THETA GROUP","S GROUP VEL"
1032 PRINT "(DEGREES)","(MM/USEC)","(DEGREES)","(MM/USEC)"
1034 PRINT
1200 FOR I=0 TO 90 STEP 5
1210 T2=I*(6.283185/360)
1215 T3(I)=T2
1220 L=COS(T2)
1230 L2=L*L
1240 M=(1-L2)**5
1250 M2=M*M
1260 H1=L2*A1+M2*A6
1270 H2=L2*A6+M2*A2
1280 H3=L*M*(A3+A6)
1290 H4=H3*H3
1300 H7=H1+H2
1310 H8=H7*H7
1320 H9=H1*H2-H4
1400 X1=0.5*(H7+(H8-4*H9)**5)
1410 X2=0.5*(H7-(H8-4*H9)**5)
1430 U1=(X2/R)**5
1600 F1=(L2*A1+M2*A6-R*U1*U1)*(2*M*A2)
1610 G1=(L2*A1+M2*A6-R*U1*U1)*(2*L*A6)
1620 F2=(L2*A6+M2*A2-R*U1*U1)*(2*M*A6)
1630 G2=(L2*A6+M2*A2-R*U1*U1)*(2*L*A1)
1640 F3=-2*M*L2*(A3+A6)**2
1650 G3=-2*L*M2*(A3+A6)**2
1660 F4=F1+F2+F3
1670 G4=G1+G2+G3
1680 U1=L2*(A1+A6)+M2*(A6+A2)-2*R*U1*U1
1690 U2=-2*R*U1
1700 U3=U1*U2
1710 U4=(F4+F4+G4+G4)/(U3*U3)
1720 U5=U4**5
1730 T7=F4/G4
1740 T8=(180/3.14159)*ATN(T7)
1770 PRINT I,U1,T8,U5
1780 NEXT I
2000 DATA 27.4,5,2.5,.26,2.52
9999 END

```

TABLE A-1. CALCULATED PLATE WAVE SPEEDS OF GY70/A201

E11 =	27.4	NSI
E22 =	5	NSI
G12 =	2.5	NSI
POISSONS RATIO =	.26	
DENSITY =	2.52	GMS/CC

FAST WAVE SPEEDS VERSUS ANGLE

THETA PHASE (DEGREES)	F PHASE VEL (MM/USEC)	THETA GROUP (DEGREES)	F GROUP VEL (MM/USEC)
0	8.71337	5.35671E-7	8.71337
5	8.6839	.556083	8.71009
10	8.59579	1.12141	8.70003
15	8.44995	1.70591	8.68262
20	8.24794	2.3209	8.65678
25	7.99196	2.9802	8.62081
30	7.68491	3.70159	8.57214
35	7.33048	4.50927	8.50689
40	6.93327	5.43812	8.41913
45	6.49904	6.54179	8.29952
50	6.03515	7.90967	8.13264
55	5.55142	9.70745	7.8913
60	5.06206	12.2915	7.52273
65	4.5902	16.5963	6.91422
70	4.17916	25.5448	5.85483
75	3.89977	45.146	4.49646
80	3.77398	67.7915	3.8613
85	3.73184	81.2612	3.7398
90	3.72217	90.0001	3.72217

SLOW WAVE SPEEDS VERSUS ANGLE

THETA PHASE (DEGREES)	S PHASE VEL (MM/USEC)	THETA GROUP (DEGREES)	S GROUP VEL (MM/USEC)
0	2.61569	8.66539E-6	2.61569
5	2.62356	8.91967	2.62971
10	2.6468	17.5449	2.66991
15	2.68425	25.6413	2.73122
20	2.73414	33.0663	2.80681
25	2.79418	39.7662	2.88961
30	2.86177	45.7506	2.97341
35	2.93409	51.0619	3.05328
40	3.00821	55.7464	3.1255
45	3.08108	59.8259	3.18719
50	3.14937	63.2574	3.2356
55	3.20903	65.8411	3.26735
60	3.25407	66.9617	3.27824
65	3.27296	64.7922	3.27298
70	3.23907	54.9962	3.25339
75	3.1858	39.8646	3.19778
80	2.88531	37.8606	3.09111
85	2.69095	53.2618	3.16411
90	2.61569	90.	2.61569

APPENDIX B

PROGRAM FOR CALCULATING LAMINA STIFFNESS COEFFICIENTS
FROM PLATE WAVE SPEEDS

The following computer program, written in BASIC, applies to the calculation of the four reduced lamina stiffness coefficients Q_{11} , Q_{22} , Q_{66} and Q_{12} when more than four experimental wave speeds have been recorded. It assumes that at each angle interrogated within the lamina both the pseudolongitudinal wave speed, V_F , and the pseudoshear wave speed, V_S , have been measured. The program is based upon a least-square-error fit of two theoretical curves, $X_F(\theta)$ and $X_S(\theta)$, to the set of experimental data, where $X = \rho V(\theta)^2$. Enter the data beginning in Step 7000 in the order: angle of the transducer with respect to the fibers, θ (degrees); X_F (GPa) obtained at this angle; X_S (GPa) obtained at this angle. The program accommodates three trial values for each of the four Q_{ij} 's and computes the square-error sum for all 81 combinations of Q_{ij} . The output lists the best five combinations in order of descending total square error; the least-square-error value, representing the best fit of the two curves simultaneously, is the final set. Enter the trial Q_{ij} 's in GPa units beginning in the Step 7000 in the order: Q_{11} ; Q_{22} ; Q_{66} ; Q_{12} . A sample of the program output is presented in Table B-1; the numbers therein are representative of B/A1. The two least-square-error velocity curves are shown with the experimental data on Figure B-1.

```

100 REM  PROGRAM TO CALCULATE PLATE QIJ PARAMETERS
110 REM  FROM SYMMETRICAL LAMB AND SH SHEAR WAVE
120 REM  SPEED DATA.  INPUT ANGLE(DEGREES),XF(GPA)
130 REM  XS(GPA).  INPUT ESTIMATED VALUES FOR
140 REM  Q11, Q22, Q66, Q12 IN GPA UNITS.
990 DIM D(100),C1(100),C2(100),C3(100),C6(100)
995 REM  N = NUMBER OF ANGLES INTERROGATED
1000 FOR N=1 TO 5
1005 READ T1(N),X1(N),X2(N)
1010 T(N)=T1(N)*(3.14159/180)
1015 NEXT N
1020 FOR N=1 TO 3
1025 READ Q1(N),Q2(N),Q6(N),Q3(N)
1030 NEXT N
1031 PRINT "TRIAL VALUES OF QIJ IN GPA UNITS"
1032 PRINT "Q11","Q22","Q66","Q12"
1033 FOR H = 1 TO 3
1034 PRINT Q1(H),Q2(H),Q6(H),Q3(H)
1036 NEXT H
1038 M=1
1040 FOR I=1 TO 3
1045 FOR J=1 TO 3
1050 FOR K=1 TO 3
1055 FOR L=1 TO 3
1058 D2 = 0
1059 REM  N = NUMBER OF ANGLES INTERROGATED
1060 FOR N=1 TO 5
1100 A1(N) = Q1(I)*(COS(T(N)))**2 + Q6(L)*(SIN(T(N)))**2
1110 A2(N) = Q6(L)*(COS(T(N)))**2 + Q2(J)*(SIN(T(N)))**2
1120 A3(N) = (Q3(K)+Q6(L)) * (SIN(T(N))*COS(T(N)))
1150 X5(N) = (A1(N)+A2(N))/2
1155 X6(N) = 0.5*(((A1(N)-A2(N))**2 + 4*A3(N)**2))**0.5
1160 X3(N) = X5(N) + X6(N)
1165 X4(N) = X5(N) - X6(N)
1180 D1(N) = (X3(N)-X1(N))**2 + (X4(N)-X2(N))**2
1190 D2=D2+D1(N)
1200 NEXT N
1210 D(N) = D2
1212 C1(N) = Q1(I)
1214 C2(N) = Q2(J)
1216 C3(N) = Q3(K)
1218 C6(N) = Q6(L)
1220 M = M+1
1245 NEXT L
1250 NEXT K
1255 NEXT J
1260 NEXT I
1400 M=1
1410 FOR I=1 TO 80
1420 K=I + 1
1430 FOR J=K TO 81
1440 IF D(I) > D(J) THEN 1500
1450 T1 = D(I)

```

```
1452 T2 = C1(I)
1454 T3 = C2(I)
1456 T4 = C3(I)
1458 T5 = C6(I)
1460 B(I) = B(J)
1462 C1(I) = C1(J)
1464 C2(I) = C2(J)
1466 C3(I) = C3(J)
1468 C6(I) = C6(J)
1470 B(J) = T1
1472 C1(J) = T2
1474 C2(J) = T3
1476 C3(J) = T4
1478 C6(J) = T5
1500 NEXT J
1510 NEXT I
1602 PRINT
1603 PRINT
1604 PRINT "BEST FIVE SETS OF QIJ (GPA)"
1605 PRINT
1606 PRINT "Q11","Q22","Q66","Q12","SQUARE ERROR"
1607 PRINT
1608 FOR I = 77 TO 81
1610 PRINT C1(I),C2(I),C6(I),C3(I),D(I)
1620 NEXT I
1680 REM ENTER ANGLE, XF, XS
7000 DATA 00,239.52,58.126
7100 DATA 20,219.21,61.055
7200 DATA 45,171.43,72.641
7300 DATA 60,163.28,71.930
7400 DATA 90,158.38,60.079
7450 REM ENTER Q11,Q22,Q66,Q12
7500 DATA 235,157,56,37.5
7600 DATA 235.5,157.5,56.5,38
7700 DATA 236,158,57,38.5
9999 END
```

TABLE B-1. REDUCED STIFFNESS COEFFICIENTS
OF B/A₂ FROM PLATE WAVE DATATRIAL VALUES OF Q_{IJ} IN GPa UNITS

Q ₁₁	Q ₂₂	Q ₆₆	Q ₁₂
235	157	56	37.5
235.5	157.5	56.5	38
236	158	57	38.5

BEST FIVE SETS OF Q_{IJ} (GPa)

Q ₁₁	Q ₂₂	Q ₆₆	Q ₁₂	SQUARE ERROR
236	157.5	56.5	37.5	90.6936
235.5	157.5	56.5	38.5	90.6852
236	157.5	56.5	38	90.6342
235.5	157.5	56.5	37.5	90.5591
235.5	157.5	56.5	38	90.4256

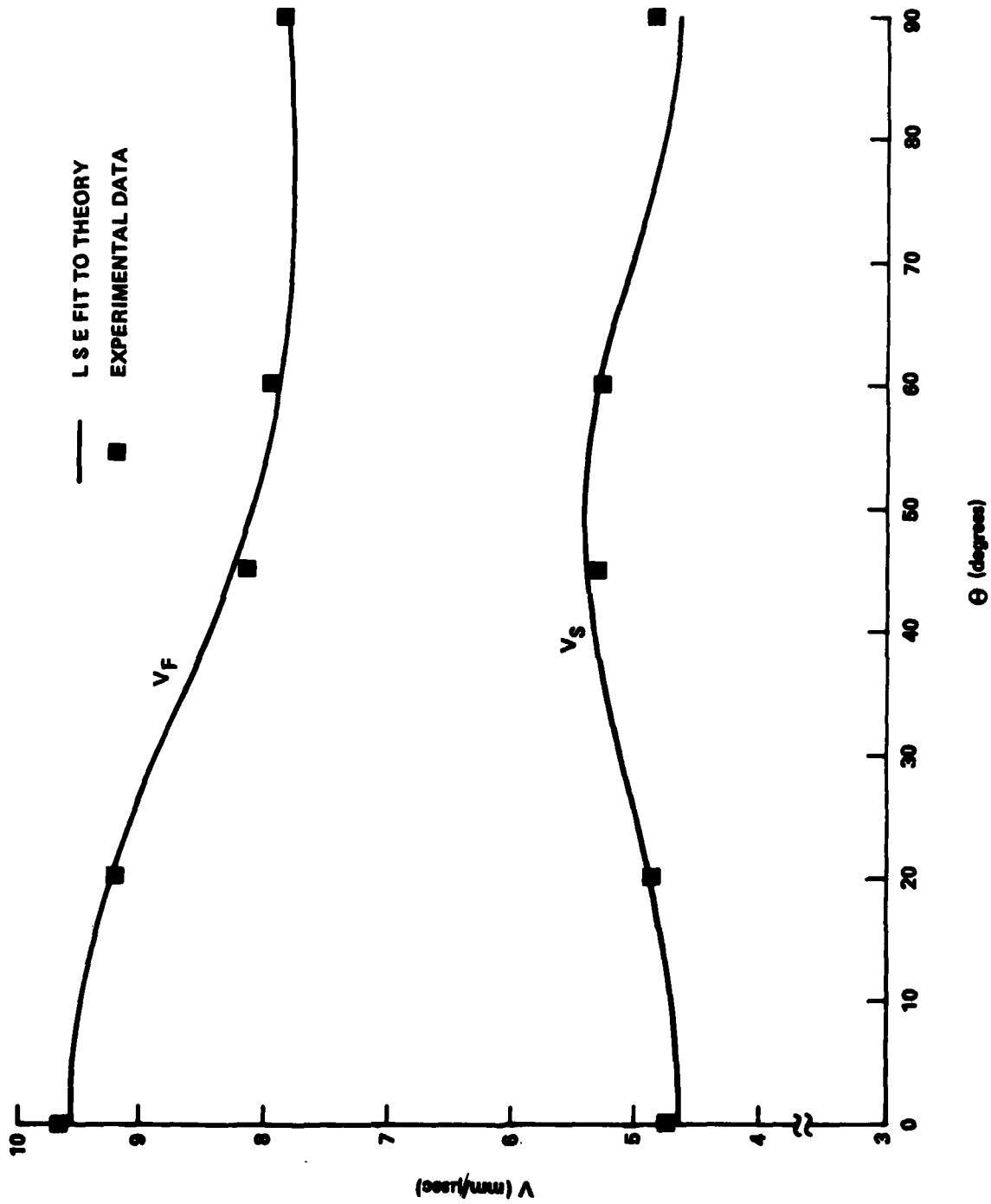


FIGURE B-1. LEAST-SQUARE-ERROR CURVES VS MEASURED PLATE WAVE SPEEDS FOR BORON/ALUMINUM

DISTRIBUTION

Copies

Defense Technical Information
Center
Cameron Station
Alexandria, VA 22314

12

Internal Distribution:

E231

9

E232

3

R30

1

R32

1

R32 (J. V. Foltz)

10

R32 (A. L. Bertram)

10

R34 (C. W. Anderson)

10

END

FILMED

11-85

DTIC